Available online at www.sciencedirect.com
ScienceDirect
Chinese Journal of Aeronautics 22(2009) 663-669
Chinese Journal of Aeronautics
www.elsevier.com/locate/cja

Microstructure-based Simulation of Plastic Deformation Behavior of SiC Particle Reinforced Al Matrix Composites

Zhang Peng, Li Fuguo*

School of Materials Science and Engineering, Northwestern Polytechnical University, Xi'an 710072, China

Received 27 October 2008; accepted 8 December 2008

Abstract

This article, in order to unearth the deformation mechanism of particle reinforced metal matrix composites, establishes a finite element model (FEM) based on the actual microstructures. It finds out and analyzes the distribution of von Mises effective stress, strain and the maximum principal stress in the matrix and particles. Moreover, the overall stress and strain in the matrix and composites are calculated. By comparison, a tiny discrepancy exists between the experimental results and the simulation with respect to flow stresses. The effects of deformation parameters, such as temperature and strain rate, on the strengthening mechanism are explored and proved to be weak.

Keywords: metal matrix composites; deformation simulation; cell model; microstructure

1. Introduction

Compared to un-reinforced metal and alloys, the particle-reinforced metal matrix composites (MMC) exhibit distinct superiority in strength, elastic modulus, wear resistance and expansion properties. Therefore, no wonder that particle-reinforced MMC have drawn enormous interest from researchers in wide production industries, such as automobile, space vehicle, aircraft, ship and sport requisites and otherwise. However, MMC always display poor ductility at room temperature due to addition of brittle ceramic particles. This makes it necessary to fabricate MMC at elevated temperatures[1-5]. At present, investigating the MMC deformation behavior through variety of experimental methods is under way; nevertheless, to clarify the effects of the shape, size and distribution of particles on MMC deformation behavior still remains one of focuses to attract most researchers' attention. As far as the measures for research are concerned, the numerical approach can be counted among the most popular ones. In the numerical simulation, most models adopt the "unit cell" conception, in which one simple-shape particle like an ellipse or a rectangle is embedded in the matrix[6-9]. This approach is deficient in that it fails to accurately predict the overall mechanical property of a true microstructure of composites thereby leading to exacerbating the analysis precision. However, to authors' knowledge, few efforts, so far, have been devoted to improvement of the cell model. To fill this void, this article introduces a new numerical model on the basis of actual microstructures to investigate the deformation mechanism at elevated temperatures.

2. Experimental

The material used for investigation was an aluminum alloy reinforced with 15% volume of silicon carbide particles with an average size of 12 μm. The material was produced by blending SiC particles and Al powder followed by compacting and hot pressing them into blanks, which were then extruded into cylinders at 1 016 K and with a ratio of 20∶1. Fig.1 shows the as-extruded microstructure, in which Fig.1(a) shows the longitudinal microstructure parallel to the extrusion axis and Fig.1(b) the transverse microstructure perpendicular to the same axis. Compared with Fig.1(b), Fig.1(a) more markedly illustrates the microstructure characteristic of band distribution with clustered particles distributing at some sites.

*Corresponding author. Tel.: +86-29-83070387.
E-mail address: fuguolx@nwpu.edu.cn
Foundation item: Aeronautical Science Foundation of China (03H53048)

doi: 10.1016/S1000-9361(08)60156-9

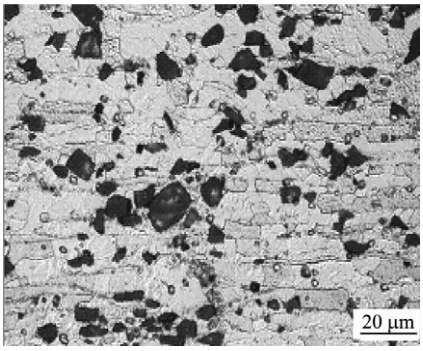

(a) Longitudinal direction

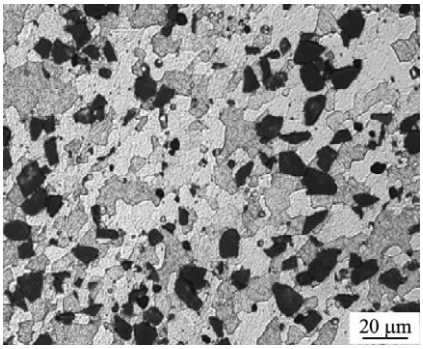

(b) Transverse direction

Fig.1 Microstructure of as-extruded MMC.

3. Finite Element Model

3.1. Cell model

In order to study the real mechanical properties, a 2D cell model is established based on the microstructure in Fig.2, as shown in Fig.3. Fig.2 displays an unevenly distributed structure out of particles of different sizes and shapes. By comparing Fig.2 with Fig.3, they are quite similar in particle shapes, distribution, size as well as particle orientation typical of the microstructure of the composites. Fig.4 shows the finite element mesh for numerical simulation, where, for convenience in analysis, the plane stress type is taken.

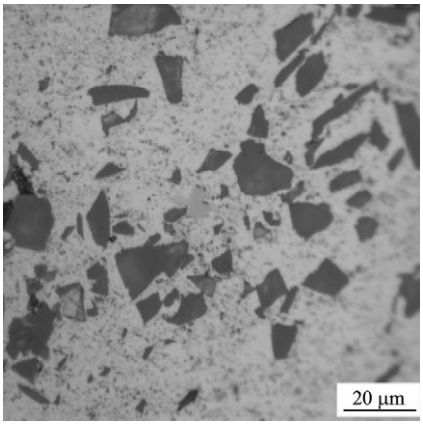

Fig.2 Microstructure taken for FEM simulation.

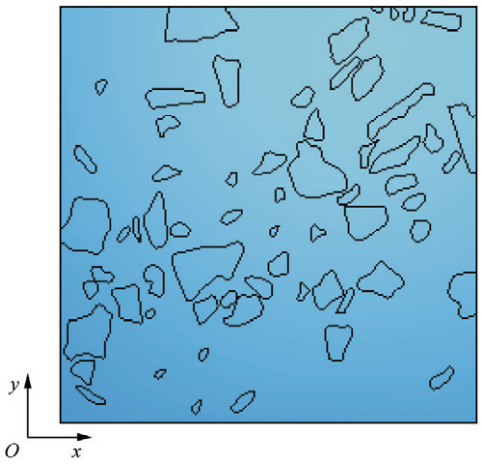

Fig.3 2D cell model.

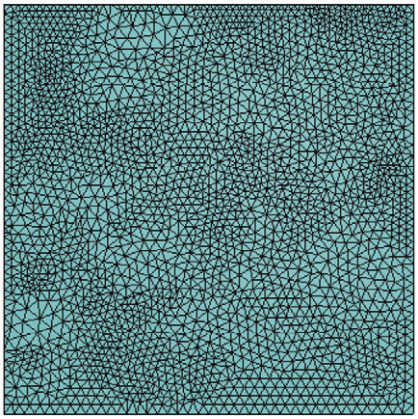

Fig.4 Finite element mesh for simulation.

3.2. Boundary condition

The boundary condition is so set that at the bottom border $U_y = 0$ and at the upper border is imposed a negative displacement load U_y in y-direction to make 30% model deform. In order to keep harmonic deformation, the order of equation in the software ABAQUS is so assumed as to make the left and right borders of the model remain straight. In deformation, the strain rates $\dot{\varepsilon}$ are supposed to be 0.01, 0.10, 1.00 s^{-1}, while the temperature $T = 713$, 733, 753, 773 K.

3.3. Material description

The SiC particles are assumed to be linearly elastic with elastic modulus $E_p = 440$ GPa and Poisson's ratio $\nu_p = 0.17$. As a hot-deformation material, 6061 Al-alloy is selected to be the metallic matrix with elastic modulus $E_m = 70$ GPa, Poisson's ratio $\nu_m = 0.33$ and the stress-strain relation[10] defined as

$$\sigma = 2.011\times10^3 \varepsilon^{0.08012} \dot{\varepsilon}^{0.08} \exp(-0.004\,84T) \quad (1)$$

3.4. Data processing

Generally, the numerical true stress-strain curves of composites in a cell model are obtained by averaging the stress and strain in it. For a composite, the overall true stress σ_e and the corresponding overall true strain ε_e in the cell model are calculated by

$$\left.\begin{aligned}\sigma_c &= \frac{1}{V_c}\left[\sum_{k=1}^{N_c}\sigma_{c,k}V_{c,k}\right]\\ \varepsilon_c &= \frac{1}{V_c}\left[\sum_{k=1}^{N_c}\varepsilon_{c,k}V_{c,k}\right]\end{aligned}\right\} \tag{2}$$

where V_c represents the total volume of the cell model, $V_{c,k}$ the volume of the kth element in the cell model, $\sigma_{c,k}$ the average true stress of the kth element in the cell model, $\varepsilon_{c,k}$ the average true strain of the kth element in the cell model, and N_c the total of elements in the cell model.

σ_m and σ_p, the average true stress components of the matrix and the particle respectively in the cell model, are determined by

$$\left.\begin{aligned}\sigma_m &= \frac{1}{V_m}\left[\sum_{i=1}^{N_m}\sigma_{m,i}V_{m,i}\right]\\ \sigma_p &= \frac{1}{V_p}\left[\sum_{j=1}^{N_p}\sigma_{p,j}V_{p,j}\right]\end{aligned}\right\} \tag{3}$$

where V_m is the total volume of the matrix, $V_{m,i}$ the volume of the ith element of the matrix, $\sigma_{m,i}$ the average true stress of the ith element of the matrix, N_m the total of elements of the matrix; V_p the total volume of the particle, $V_{p,j}$ the volume of the jth element of the particle, $\sigma_{p,j}$ the average true stress of the jth element of the particle, and N_p the total of elements of the particle.

4. Results and Discussion

4.1. Stress and strain distribution

Hereafter, the test results acquired at the temperature $T = 733$ K and the strain rate $\dot{\varepsilon} = 0.01\ s^{-1}$ are chosen to be the example to introduce the deformation behavior of the composites. Fig.5 illustrates the contour plots of von Mises effective stress in aluminum matrix with different deformation degrees for the 15% SiC_p/Al composites. It is noted that the distribution of von Mises effective stress in the matrix appears very inhomogeneous during 10% and 20% deformations due to the mismatch of elastic modulus between the particles and the matrix. Simultaneously, the maximum von Mises effective stress in matrix distributes along the band oriented 45° to the loading axis in line with the maximum shear stress direction. From Fig.5, it is observed that the von Mises effective stress in the y-direction is greater than in the x-direction, and the von Mises effective stress around the particle in the x-direction seems to distribute in a gradient form. Meanwhile, the von Mises effective stress at the sharp corners of particles always zooms up as a result of stress concentration. In further deformation, the plastic zone enlarges and when reaching 30%, it becomes evident that the von Mises effective stress has already distributed in the matrix uniformly except in some regions where exist larger particles. This implies that the neighboring larger particle would place stronger constraints on the matrix in deformation.

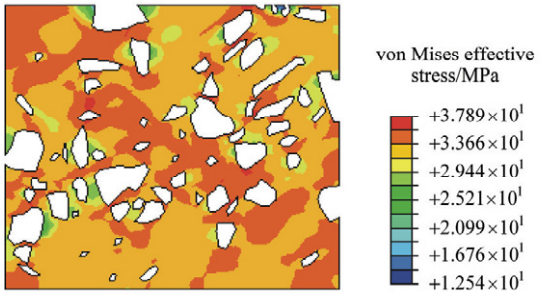

(a) 10%

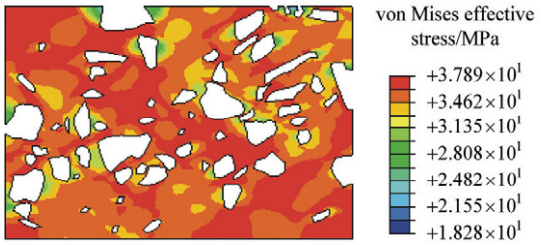

(b) 20%

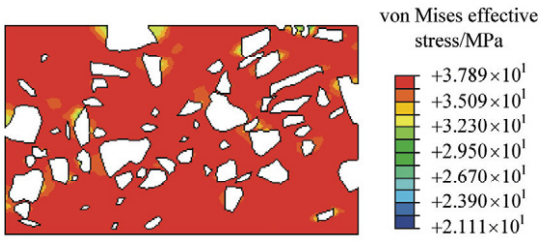

(c) 30%

Fig.5 von Mises effective stress in matrix.

Fig.6 shows the contour plots of von Mises effective stress in deformed particles. It is noticeable that the von Mises effective stress in particles is greater than those in the matrix, which indicates obvious strengthening effects. Compared Figs.6(a)-6(c), it is clear that only few particles present greater von Mises effective stress when 10% deformed, and only at particles' sharp corners turns up the maximum von Mises effective stress. With further deformation, von Mises effective stress in particles tends to distribute more evenly, but still less than in the matrix.

Fig.7 shows the distribution of effective plastic strain in the deformed matrix. It should be pointed out that there is a maximum plastic strain zone along the band oriented 45° to the loading axis. The plastic strain

around the particles in the *y*-direction is greater than in the *x*-direction. Besides, in the neighboring particles, with further deformation, the strain fields tend to get merged with each other, which indicate the distances of particles would exert influence upon the deformation of matrix.

Fig.8 shows the distribution of the maximum principal stress in the matrix. It is evident that the positive principal stress appears on both sides around the particles, which evidences there to be tensile stresses during deformation especially in the neighboring particles.

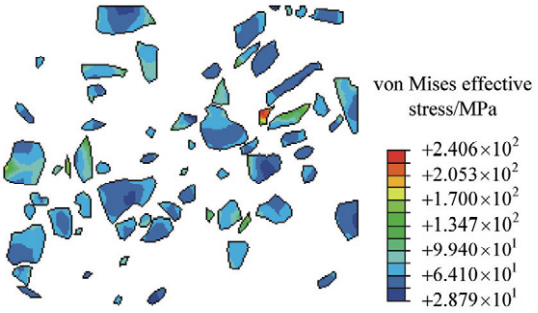

(a) 10%

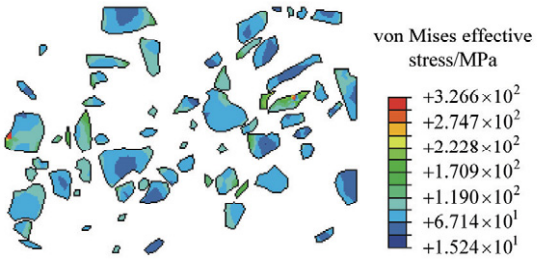

(b) 20%

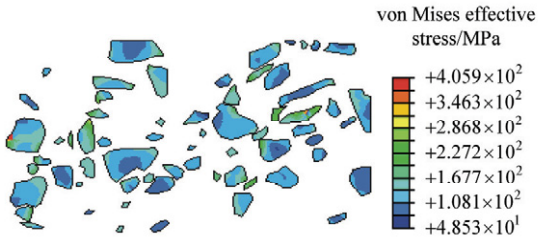

(c) 30%

Fig.6 von Mises effective stress in particles.

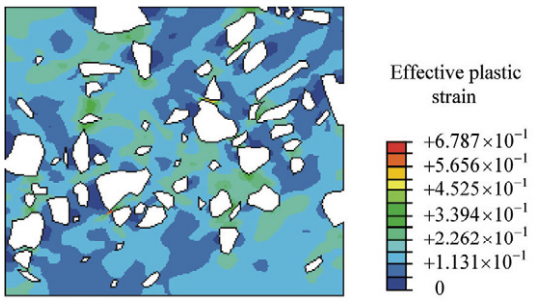

(a) 10%

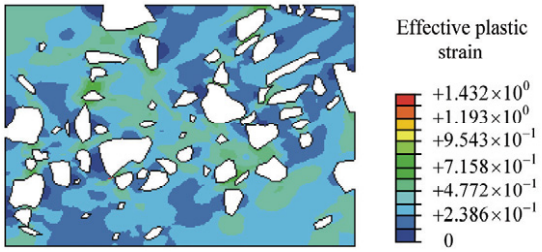

(b) 20%

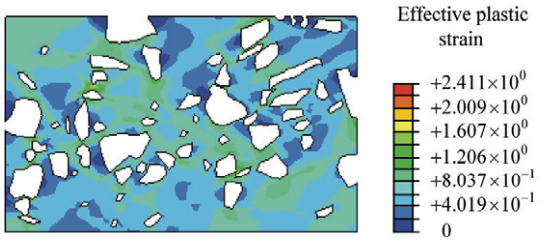

(c) 30%

Fig.7 Effective plastic strain in matrix.

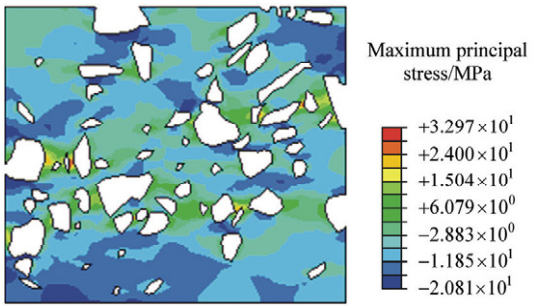

(a) 10%

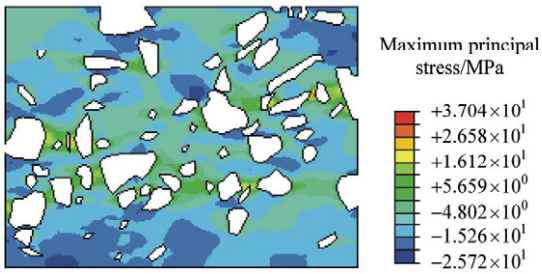

(b) 20%

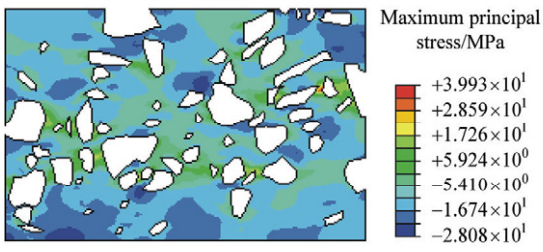

(c) 30%

Fig.8 Maximum principal stress in matrix.

Fig.9 shows the distribution of maximum principal stresses in the particles. It is noteworthy that the positive principal stress emerges on the upper or bottom surfaces of particles rather than at right or left sides.

This might be ascribed to the flow of matrix that induces the shear stress in the interface between the matrix and particles. Particle fracture is often blamed for large tensile principal stress[11]. Therefore, Fig.9 can be used to predict which particle would suffer fracture during deformation.

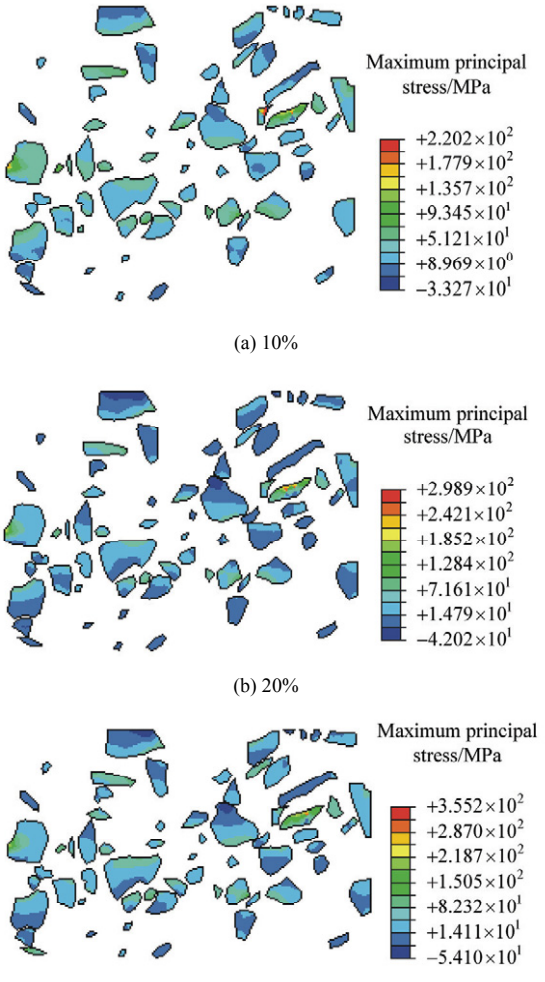

Fig.9 Maximum principal stress in particles.

4.2. Flow stress-strain curves of matrix and composites

Eqs.(2)-(3) define the flow stress and strain of the matrix and composites. Based on them, Fig.10 shows the variation of average matrix stress σ_m as a function of the model's overall strain ε_c with different parameters. Clearly, a good agreement exists between the curves from both simulation and the experiments with a discrepancy within 3%.

Fig.11 shows the variation of average composite stress σ_c against the model's overall strain ε_c in the case of different parameters. Contrary to Ref.[5], the differences in the results between the simulation and the experiments are minor and, if any, they present themselves more in the appearance than in what else. As far as the yield stress is concerned, in simulation it increases all the time, but concerning the increase of strain, the trend of its increase is weakening. In contrast, Ref.[5] disclosed that stress stays almost unchanged with increase of strain after the yield stress. One reason responsible for the difference might be the material property of SiC particles that is assumed to be of linear elasticity. As a result, in simulation, to keep consistent with the experimental results in the matrix, the stress in the particles should always increases thereby unavoidably increasing in the composites all along. The other reason might be for the existence of stress limit in the particles in actual deformation, which would cause particles crashing once the stress reaches the limit and results in stress declining in particles. One way and another, both reasons make the composite stresses in simulation to deviate from those in experiments. Anyhow, the results from the simulation would bring no effects upon the deformation analysis. By comparing Fig.10 with Fig.11, it is evident that composites have greater flow stress than the matrix has, which is a testament to the great strengthening effects the particles have given birth to.

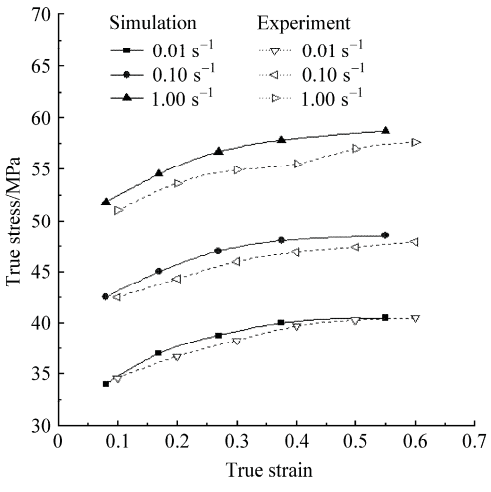

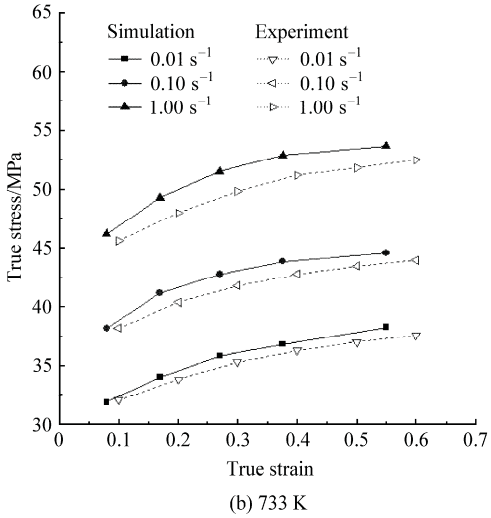

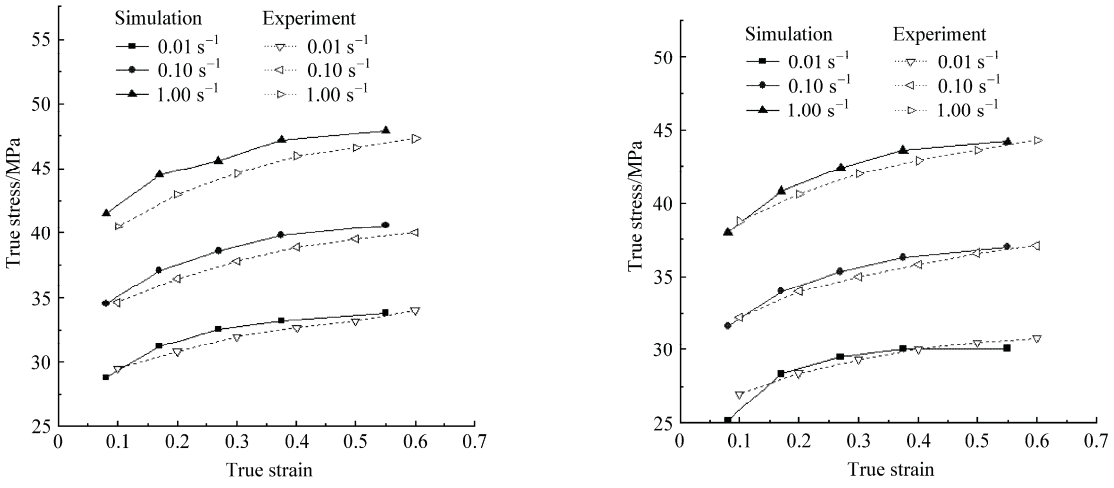

(c) 753 K (d) 773 K

Fig.10 Flow stress-strain curves for matrix.

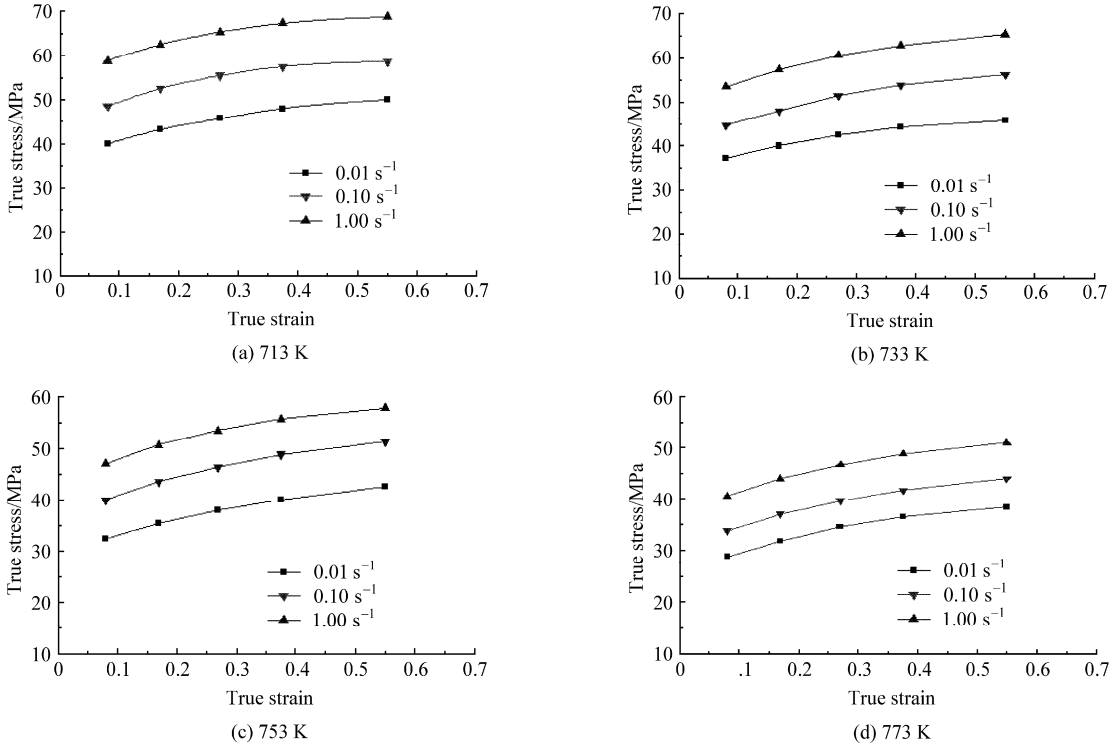

(a) 713 K (b) 733 K

(c) 753 K (d) 773 K

Fig.11 Flow stress-strain curves for composites.

4.3. Strengthening mechanism

Generally, there are two types of strengthening mechanism in MMC: direct and indirect. The direct strengthening results from the load transferring from the matrix to the particles owing to the particles having a much higher elastic module than the matrix while the indirect strengthening from the influences that the particles might exert on the matrix microstructure or deformation mode. In order to further unearth the strengthening mechanism in the case of different parameters, a parameter ratio σ_c/σ_m is adopted under the same strain to express the stress partition. It can be seen from the ratio that the greater the ratio is, the more obvious the strengthening effect is. Otherwise, the effect turns weak.

In order to clarify the effects of temperature and strain rate on the strengthening, the results acquired at temperature 713 K and strain rate 0.10 s^{-1} are taken as an example to analyze. Fig.12 shows the curves of σ_c/σ_m vs ε_c. It is clear that with ε_c increasing, the value of ratio shows a monotonic increase, but at the same strain ε_c, the temperature and the strain rate have minor effects. This leads to an inference that the deformation condition exerts insignificant influences on the strengthening.

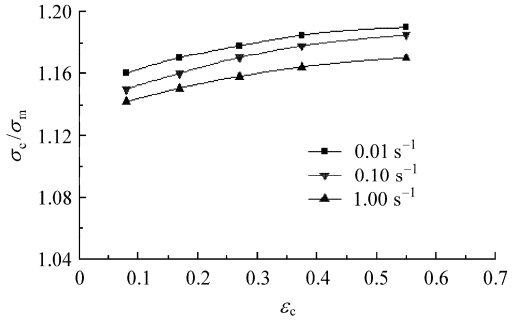

(a) 713 K

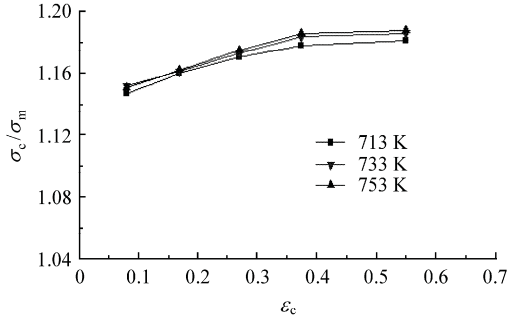

(b) 0.10 s^{-1}

Fig.12 Curves of σ_c/σ_m vs ε_c.

5. Conclusions

(1) The 2D cell model based on the actual microstructure is established to investigate the large plastic deformation at elevated temperatures. In the analysis, the von Mises effective stress, strain and maximum principal stress in the matrix and particles are defined and investigated.

(2) The predicted stress-strain behavior of the composites from simulation is qualitatively consistent with the experimental results.

(3) Analysis of the strengthening effects in the case of different deformation parameters reveals that strain rate and temperature play a minor role in affecting strengthening behavior.

References

[1] Srivastava V C, Jindal V, Uhlenwinkel V. Hot-deformation behaviour of spray-formed 2014 Al+SiC_p metal matrix composites. Materials Science and Engineering: A 2008; 477(1-2): 86-95.

[2] Ramanathan S, Karthikeyan R, Ganasen G. Development of processing maps for 2124 Al/SiC_p composites. Materials Science and Engineering: A 2006; 441(1-2): 321-325.

[3] Cavaliere P, Evangelista E. Isothermal forging of metal matrix composites: recrystallization behaviour by means of deformation efficiency. Composites Science and Technology 2006; 66(2): 357-362.

[4] Cavaliere P, Cerri E, Leo P. Hot deformation and processing maps of particulate reinforced 2618/Al_2O_3/20p metal matrix composite. Composites Science and Technology 2004; 64(9): 1287-1291.

[5] Ganesan G, Raghukandan K, Karthikeyan R, et al. Development of processing maps for 6061 Al/15% SiC_p composite material. Materials Science and Engineering: A 2004; 369(1-2): 230-235.

[6] Zhang W X, Li L, Wang T J. Interphase effect on the strengthening behavior of particle-reinforced metal matrix composites. Computational Materials Science 2007; 41(2): 145-155.

[7] Yan Y W, Geng L, Li A B. Experimental and numerical studies of the effect of particle size on the deformation behavior of the metal matrix composites. Materials Science and Engineering: A 2007; 448(1-2): 315-325.

[8] Xu N, Zong Y P, Zhang F. Simulation of stress in reinforcements and stress-strain curve of SiC_p/Al-2618 matrix composite. Acta Metallurgica Sinica 2007; 43(8): 863-867. [in Chinese]

[9] Yu J Y, Li Y L, Zhou H X. Influence of particle size on the dynamic behavior of PMMCS. Acta Materiae Compositae Sinica 2005; 22(5): 31-38. [in Chinese]

[10] Zhao P F, Ren G S, Shen Z. Influence of hot compressive deformation conditions of 6061 aluminum alloy on stress and research on its constitutive equation. Journal of Plasticity Engineering 2007; 14(6): 130-133. [in Chinese]

[11] Shen H, Lissenden C J. 3D finite element analysis of particle-reinforced aluminum. Materials Science and Engineering: A 2002; 338(1-2): 271-281.

Biographies:

Zhang Peng Born in 1977, now he is a Ph.D. candidate in School of Materials Science and Engineering, Northwestern Polytechnical University. His major research fields are materials processing engineering, simulation and control of material deformation.
E-mail: pezhan@163.com

Li Fuguo Born in 1965, he is a professor in School of Materials Science and Engineering, Northwestern Polytechnical University. His major research fields are materials processing engineering, numerical simulation and date integration.
E-mail: fuguolx@nwpu.edu.cn